Topological feature and phase structure of QCD at complex chemical potential

AUTHOR(S):

Kashiwa, Kouji; Ohnishi, Akira

CITATION:

Kashiwa, Kouji ...[et al]. Topological feature and phase structure of QCD at complex chemical potential. Physics Letters, Section B: Nuclear, Elementary Particle and High-Energy Physics 2015, 750: 282-286

ISSUE DATE:

2015-11-12

URL:

http://hdl.handle.net/2433/217335

Physics Letters B 750 (2015) 282–286

Contents lists available at ScienceDirect

Physics Letters B

www.elsevier.com/locate/physletb

Topological feature and phase structure of QCD at complex chemical potential ☆

Kouji Kashiwa *, Akira Ohnishi

Yukawa Institute for Theoretical Physics, Kyoto University, Kyoto 606-8502, Japan

ARTICLE INFO

Article history:
Received 9 June 2015
Received in revised form 4 September 2015
Accepted 15 September 2015
Available online 19 September 2015
Editor: J.-P. Blaizot

Keywords:
QCD phase diagram
Deconfinement transition
Complex chemical potential

ABSTRACT

The pseudo-critical temperature of the confinement–deconfinement transition and the phase transition surface are investigated by using the complex chemical potential. We can interpret the imaginary chemical potential as the Aharonov–Bohm phase, then the analogy of the topological order suggests that the Roberge–Weiss endpoint would define the pseudo-critical temperature. The behavior of the Roberge–Weiss endpoint at small real quark chemical potential is investigated with the perturbative expansion. The expected QCD phase diagram at complex chemical potential is presented.

1. Introduction

Understanding of the phase structure of Quantum Chromodynamics (QCD) is one of the most important and interesting subjects in nuclear and elementary particle physics. The lattice QCD simulation is a powerful and gauge invariant method, but it has the sign problem at finite real chemical potential (μ_{R}), and we cannot obtain reliable results at large μ_{R}. Some methods are proposed to circumvent the sign problem, see Ref. [1] as an example, but those methods are limited in the $\mu_{\mathrm{R}}/T < 1$ region where T is temperature. Because of the sign problem, low energy effective models of QCD are extensively used to explore the QCD phase diagram. Effective models, however, have strong ambiguities and thus quantitative predictions are impossible at present. Towards unification of lattice QCD simulations and effective model approaches, a new method so-called *imaginary chemical potential matching approach* [2,3] is proposed recently. In this method, we use lattice QCD data obtained at finite imaginary chemical potential (μ_{I}) to constrain effective models. It is well known that the sign problem does not exist in the finite μ_{I} region and the region has information on the μ_{R} region; constrained models are reliable not only at finite μ_{I} but also at finite μ_{R}.

In addition to the imaginary chemical potential matching approach, the concept of the imaginary chemical potential may be important to define the confinement–deconfinement transition. In the imaginary time formalism where its time direction is compactified, the imaginary chemical potential can be interpreted as the Aharonov–Bohm phase induced by $U(1)$ flux insertions to the closed time loop. From this interpretation, we can determine the pseudo-critical temperature of the deconfinement transition from the Roberge–Weiss (RW) endpoint [4] with an analogy of the topological order [5,6] as explained later.

It is also interesting to investigate the phase structure at *finite complex* chemical potential, $\mu = \mu_{\mathrm{R}} + i\mu_{\mathrm{I}}$, where $\mu_{\mathrm{R}} \neq 0$ and $\mu_{\mathrm{I}} \neq 0$. On the (T, μ_{R}) plane ($\mu_{\mathrm{I}} = 0$), the first order phase transition may exist, then we would have the critical point (CP) as the endpoint of the first order phase transition boundary. On the (T, μ_{I}) plane ($\mu_{\mathrm{R}} = 0$), the first order RW transition line exists, and the RW endpoint can either be of the first or of the second order. Some lattice QCD simulations [7–9] suggest that the order of the RW endpoint is the first order at the physical pion mass. Then the RW endpoint is a triple point, with two other first order lines departing from the RW transition line. The first order lines appear around the heavy quark limit as well as around the chiral limit [7,9]. These lines with small quark mass may have the chiral transition nature and are referred to as the *chiral critical* lines. One of the chiral critical lines extending in the $\mu_{\mathrm{I}} \to 0$ direction should have an endpoint (chiral critical endpoint; CCE) before reaching the $\mu_{\mathrm{I}} = 0$ as long as the $\mu = 0$ transition is crossover. Fig. 1 summarizes our current expectation of the QCD phase diagram. Now we can raise a question. How does CCE behave at complex chemical potential? Specifically, is CCE on the (T, μ_{I}) plane connected with CP on the (T, μ_{R}) plane at complex chemical potential, *i.e.* in the

☆ Report number: YITP-15-45.

* Corresponding author.
E-mail address: kouji.kashiwa@yukawa.kyoto-u.ac.jp (K. Kashiwa).

http://dx.doi.org/10.1016/j.physletb.2015.09.036

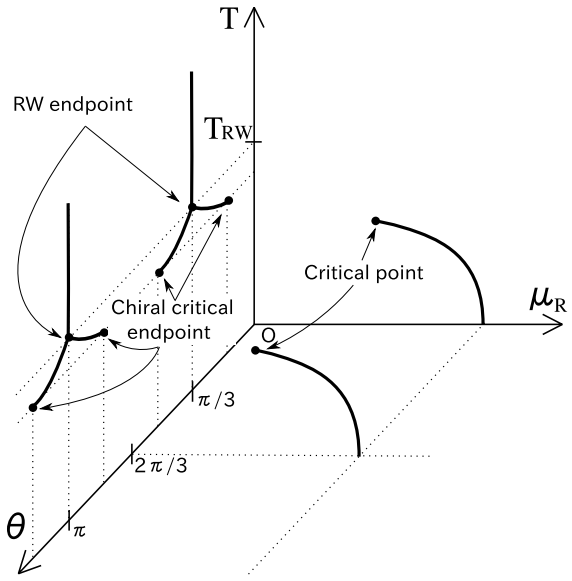

Fig. 1. Schematic figure of our current expectation of the QCD phase diagram at finite μ_R and μ_I, respectively. Solid lines represent the first order transition line.

(T, μ_R, μ_I) space? The topology of the phase diagram at complex chemical potential would tell us the relation between the deconfinement and the chiral transition.

In this letter, first we briefly summarize properties of QCD at finite imaginary chemical potential, and propose a new definition of the pseudo-critical temperature of the deconfinement transition by the RW endpoint temperature (T_{RW}). Next, we investigate the behavior of the RW endpoint at small μ_R by using the perturbative expansion. Finally, we present two scenarios of the QCD phase diagram at complex chemical potential based on the behavior of the RW endpoint at small μ_R and a symmetry argument.

2. QCD with imaginary chemical potential

At finite μ_I, QCD has a special periodicity so-called the RW periodicity [4]. The RW periodicity can effect the first order transition lines (RW transition lines) and their endpoints (RW endpoints). Those are predicted by using the strong coupling QCD and the perturbative one-loop effective potential with a background gauge field. The RW periodicity can be seen from the relation of the grand-canonical partition function Z [4]:

$$Z(\theta) = Z\left(\theta + \frac{2\pi k}{3}\right), \tag{1}$$

where a dimensionless quark imaginary chemical potential is defined as $\theta \equiv \mu_I/T \in \mathbb{R}$ and k is any integer. If quarks are confined, physical states are classified by hadron degrees of freedom unlike the deconfined phase. In the confined and deconfined phases, origins of the RW periodicity are different:

Confined phase The origin is the dimensionless baryon chemical potential 3θ in the form of $\exp(\pm 3i\theta)$ in the partition function. It can be easily seen, for example, from the strong coupling limit of the lattice QCD with the mean-field approximation [10,11], the chiral perturbation theory with the relativistic Virial expansion [12] and that with the finite energy sum rule [13].

Deconfined phase The origin is the quark chemical potential and the gauge field in the form of $\exp[\pm i(gA_4/T + \theta)]$. It generates color non-singlet contributions in the partition function. It can be understood from the perturbative one-loop effective potential with the background gauge field [14,15], and the RW periodicity is induced by $\mathbb{Z}_3$ images [4]. Then, we can find the nontrivial degeneracy of the free energy minima.

The first order RW transition lines at $\theta = \pi(2k+1)/3$ are induced by $\mathbb{Z}_3$ images. Its endpoint which is nothing but the RW endpoint should exist. The order of the RW endpoint is still under debate, but some lattice QCD simulations [7–9] suggest that the order seems to be first order around the physical pion mass.

3. Imaginary chemical potential and Aharonov–Bohm phase

In the imaginary time formalism where the temporal direction is compactified, the $U(1)$ flux can be inserted to the closed loop of the temporal coordinate. Then, the imaginary chemical potential can be regarded as the Aharonov–Bohm phase [16]. The Aharonov–Bohm effect has been discussed in the spatial loop with the flux insertion. In the imaginary time formalism, the temporal coordinate shares almost the same features as the spatial coordinates and thus we can use this interpretation. In this interpretation, we may use the discussion of the topological order [5]. Actual applications to zero temperature QCD was discussed in Ref. [6]. It should be noted that the Polyakov-loop (Φ) is usually used to discuss the deconfinement transition. The Polyakov-loop can be obtained from a holonomy which is the gauge invariant integral along the temporal coordinate loop. The Polyakov-loop is the order parameter of the center symmetry breaking and it is related with the deconfinement transition in the infinite quark mass limit. The nontrivial degeneracy of the free energy minima in the deconfined phase may have some relation to the complex phase of the Polyakov-loop. It can be probed by the insertion of the flux as discussed below.

In Ref. [6], the author considered the torus T^3 at zero temperature, and introduced three adiabatic operations: (a) Insert the $U(1)$ flux to spatial closed loops, (b) exchange i-th and $i+1$-th quarks and (c) move a quark along loops. Commutation relations of the operations (b) and (c) are described by the Braid group, and the Aharonov–Bohm effect determines the commutation relations of those with (a). If quarks are deconfined, operations become non-commutable because of the quark's fractional charge. It is commutable if quarks are confined because physical states are described by hadron degrees of freedom with integer charges. Therefore, if there is only one vacuum in the deconfined phase, it is inconsistent with the non-commutability of the operations and thus vacuum degeneracy should exist.

At finite temperature, the topological order cannot be well defined, because thermal states are constructed by a mixture of pure states with the Boltzmann factor, and we cannot operate (a), (b) and (c), adiabatically. Nevertheless, the RW periodicity shows significantly different behaviors in the confined and deconfined phases as already mentioned, and it is induced by the nontrivial appearance of the RW periodicity in the deconfined phase. This fact suggests that we can distinguish the confined and deconfined phases at $\mu_I = 0$ from the non-trivial degeneracy of the effective potential at $\theta = \pi/3$. We here consider the $U(1)$ flux insertion of $2\pi/3$ to the temporal loop at zero μ_I. This corresponds to changing the $U(1)$ flux from $-\pi/3$ to $\pi/3$ at $\theta = \pi/3$. These two states are free energy minima at $\theta = \pi/3$ degenerated at $T > T_{RW}$, while they belong to the same minimum at $T < T_{RW}$. Thus the gluon configurations in states at $\theta = \pi/3$ are essentially the same as those at $\theta = 0$. This degeneracy seems similar to the vacuum degeneracy in zero T systems and the analogy can be found; the response of hidden local minima by the flux insertion via μ_I tells us the non-trivial degeneracy of the free energy minima. Therefore,

we propose that $T_{\rm RW}$ is the pseudo-critical temperature of the deconfinement transition.

Let us examine if $T_{\rm RW}$ provides a deconfinement temperature reasonably well. It should be noted that the present definition and the standard definition determined by using the Polyakov-loop are consistent in the infinite quark mass limit where the Polyakov-loop is the exact order-parameter of the deconfinement transition. Therefore, we can find the relation $T_{\rm D} = T_\Phi = T_{\rm RW}$ where T_Φ is the critical temperature determined by the susceptibility of the Polyakov-loop and $T_{\rm D}$ is the deconfinement critical temperature. When the dynamical quark is taken into account, T_Φ becomes the pseudo-critical temperature. The upper bound of the pseudo-critical temperature can be determined by using the appearance of local minima of the effective potential as found in the perturbative one-loop effective potential in the Re Φ–Im Φ plane. We call it $T_{\mathbb{Z}_3}$. From the lattice QCD and effective model predictions [17,18], we can have the relation $T_\Phi \leq T_{\rm RW} \leq T_{\mathbb{Z}_3}$. While the Polyakov-loop is no longer the exact order parameter and thus the determination of $T_{\rm D}$ is not unique, $T_{\rm RW}$ is uniquely determined. Thus, $T_{\rm RW}$ which agrees with $T_{\rm D}$ in the infinite quark mass limit is unambiguously determined in the lattice QCD and effective models and provides a reasonable value as $T_{\rm D}$ with the dynamical quark. If we adopt $T_{\rm RW}$ as $T_{\rm D}$, we lead to an implication that the deconfinement transition is the topological phase transition.

4. Roberge–Weiss endpoint at complex chemical potential

We now discuss the $\mu_{\rm R}$-dependence of the pseudo-critical temperature of the deconfinement defined by $T_{\rm RW}$. We here give a model independent argument based on the perturbative expansion of the effective potential in $\mu_{\rm R}$ as a first step to investigate the $\mu_{\rm R}$-dependence of the RW endpoint. It should be noted that non-perturbative model approaches have several difficulties. One of the promising effective models is the Polyakov-loop extended Nambu–Jona-Lasinio (PNJL) model [19]. The PNJL model has the model sign problem at finite $\mu_{\rm R}$ [20]. There are some proposals to circumvent the model sign problem, for example the complex integral path contour [21–23] based on the Lefschetz thimble [24–26] and the complex Langevin method [27,28]. Unfortunately those approaches cannot be directly used at finite complex chemical potential because we cannot maintain the RW periodicity and some other desirable properties of QCD.

The effective potential at small $\mu_{\rm R}$ is expanded to $\mu_{\rm R}^2$ order as

$$\begin{aligned}&\mathcal{V}(T,\mu_{\rm R},\mu_{\rm I})\\&= \mathcal{V}(T,0,\mu_{\rm I}) - \left(\frac{\mu_{\rm R}}{T}\right)(Tn_q(\mu_{\rm R},\mu_{\rm I})|_{\mu_{\rm R}=0})\\&-\frac{1}{2}\left(\frac{\mu_{\rm R}}{T}\right)^2\frac{d[Tn_q(\mu_{\rm R},\mu_{\rm I})]}{d\mu_{\rm R}/T}\Big|_{\mu_{\rm R}=0}+\mathcal{O}\Big((\mu_{\rm R}/T)^3\Big)\end{aligned} \tag{2}$$

where

$$T\frac{dn_q}{d\mu_{\rm R}/T}\Big|_{\mu_{\rm R}=0} = T\frac{dn_q}{d(i\mu_{\rm I}/T)}\Big|_{\mu_{\rm R}=0} = -iT\frac{dn_q}{d\theta}\Big|_{\mu_{\rm R}=0}. \tag{3}$$

Equation (3) is real, and the second term on r.h.s. of Eq. (2) should be pure imaginary.

We here neglect the imaginary part of the effective potential. This assumption corresponds to the phase quenched approximation. If the RW endpoint is of the weak first order, the n_q gap at $T_{\rm RW}$ is small and the sign problem is mild, then the phase quenched approximation is justified. If the RW endpoint is of the strong first order, the partition function at given (T,μ) is dominated by one classical vacuum, then the role of the imaginary part, or the phase of the state, is minor. The phase quenched approximation cannot be applied to the second order RW endpoint. Fortunately, the RW endpoint with the realistic quark mass is predicted to be of the first order by lattice QCD simulations [7–9] and it would be possible to ignore the imaginary part of the effective potential. Effects of the imaginary part of the effective potential will be discussed elsewhere.

Next, we consider the confinement and deconfinement configurations. We call the configuration at $(T_{\rm RW}-\epsilon)$ *confinement configuration* which is labeled as $\mathcal{C}_{-\epsilon}$ where ϵ is a infinitesimal positive value. Also, we call the configuration at $(T_{\rm RW}+\epsilon)$ *deconfinement configuration* which is labeled as $\mathcal{C}_{+\epsilon}$.

By comparing Re $\mathcal{V}$ with $\mathcal{C}_{-\epsilon}$ to that with $\mathcal{C}_{+\epsilon}$ in the $\epsilon\to 0$ limit, we can distinguish whether $T_{\rm RW}$ decreases or increases if we can estimate the third term of Eq. (2). For example in the lattice QCD and effective model calculations [29,2], we can see that Eq. (3) is negative below $T_{\rm RW}$ and it becomes moderate above $T_{\rm RW}$. The $\mu_{\rm R}^2$ correction term makes Re $\mathcal{V}$ with $\mathcal{C}_{-\epsilon}$ higher than that with $\mathcal{C}_{+\epsilon}$ because the $\mu_{\rm R}^2$ correction term is then positive with $\mathcal{C}_{+\epsilon}$. This means that the first-order $T_{\rm RW}$ decreases with increasing $\mu_{\rm R}$ at least in the small $\mu_{\rm R}$ region. This behavior is consistent with the decreasing behavior of the pseudo-critical temperature of deconfinement transition defined by using usual determinations; for example, see Refs. [19,30,31].

5. QCD phase diagram at complex chemical potential

By taking into account our perturbative result and the symmetry argument, we can sketch expected QCD phase diagrams at finite complex chemical potential. Phase diagrams expected from our present discussions are summarized in Fig. 2. Because of the RW periodicity, the phase structure should be periodic along the θ axis.

The RW transition line on the (T,θ) plane $(\mu_{\rm R}=0)$ may be topologically connected with the first order phase transition boundary on the $(T,\mu_{\rm R})$ plane $(\theta=0)$. Two of the first order transition lines starting from the RW endpoint have chiral transition nature and are referred to as the *chiral transition lines* [7]. Then it is not unreasonable to expect that the endpoint of the chiral critical line on the (T,θ) plane is connected with the QCD critical point on the $(T,\mu_{\rm R})$ plane. In this case, the first order phase boundary on the $(T,\mu_{\rm R})$ plane forms a chiral transition surface in the $(T,\mu_{\rm R},\theta)$ space, and connects the $(T,\mu_{\rm R})$ plane and the (T,θ) plane. The RW transition line extends in the finite $\mu_{\rm R}$ region and forms an RW transition surface in the $(T,\mu_{\rm R},\theta)$ space. The RW endpoint may reach $T=0$ as shown in the top panel of Fig. 2 or it may deviate from the chiral transition surface at some temperature. It is deeply related with a strength of the correlation between the chiral transition surface and the RW transition surface.

Another possibility is that the first order transition lines on the (T,θ) plane are topologically separated from the first order phase boundary on the $(T,\mu_{\rm R})$ plane, as shown in the bottom panel of Fig. 2. $T_{\rm RW}$ first decreases at small $\mu_{\rm R}$, but does not reach the chiral transition surface. In this case, the deconfinement transition represented by the RW endpoint on the (T,θ) plane has less relevance to the first order phase boundary, which would be the chiral transition, on the $(T,\mu_{\rm R})$ plane. Therefore, we can call this possibility *uncorrelated case* and the former possibility *correlated case*.

The QCD phase diagram at finite complex chemical potential is related with the following subjects. (I) In Refs. [32,33], the authors use experimental data to construct the canonical partition function. Then, $T_{\rm RW}$ at $\mu_{\rm R}=0$ is used to clarify realized temperatures in experiments through the Lee–Yang zero analysis [34,35]. In the analysis, $T_{\rm RW}$ at finite $\mu_{\rm R}$ should be related with zeros inside the unit circle on the complex quark fugacity plane. If so, there is the possibility that we can strictly determine realized temperatures in experiments if we can systematically understand the

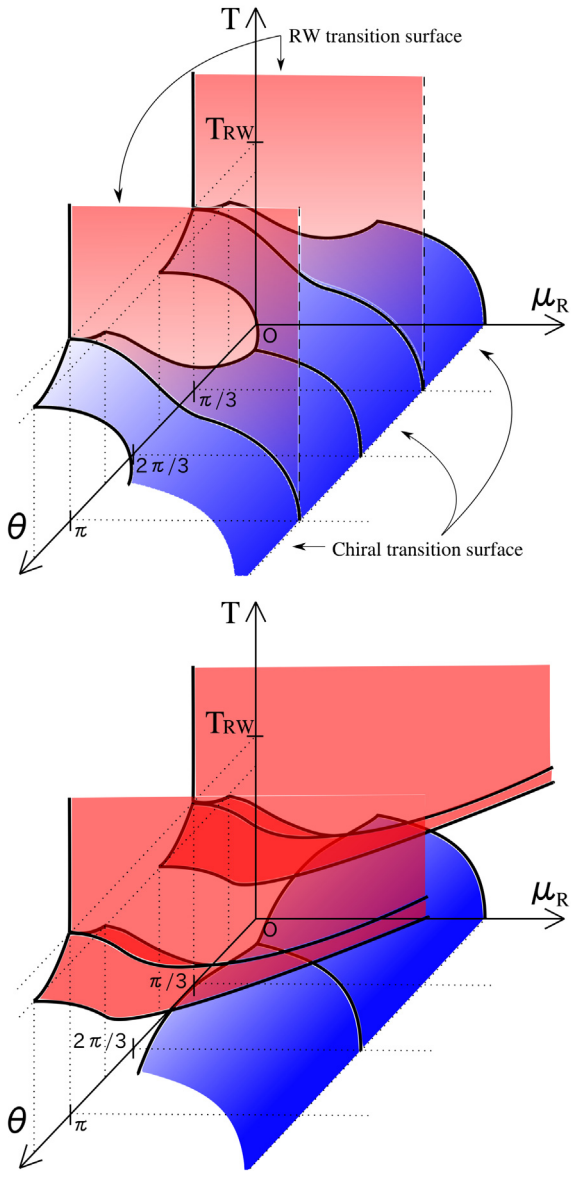

Fig. 2. Two possible schematic QCD phase diagrams at finite complex chemical potential. The top (bottom) panel represents the correlated (uncorrelated) case between the chiral and RW transition surfaces.

behavior of zeros. (II) The analytic continuation in QCD from the imaginary to the real chemical potential is usually performed on the μ^2 plane. In the continuation, we may miss some information such as an inhomogeneous condensate [36]. The analytic continuation on the complex chemical potential plane may restore the information missing.

6. Summary

We have proposed that the Roberge–Weiss endpoint provides a reasonable deconfinement temperature. The imaginary chemical potential can be interpreted as the Aharonov–Bohm phase induced by $U(1)$ flux insertions and then the analogy of the topological order can be used. In the deconfined phase, we can probe the degeneracy of the free energy by inserting the $U(1)$ flux, and these states belong to different minima. On the other hand, in the confined phase, we cannot find such non-trivial structure of the free energy. This suggests that we can distinguish the confined and deconfined phases at $\theta = \mu_I/T = 0$ from the hidden non-trivial degeneracy of the effective potential. Then, T_{RW} becomes the pseudo-critical temperature at $\mu = 0$.

In this study, we have used the analogy of the topological order at finite T. The topological transition does not have the usual order parameter, but a relation with an entanglement and topological entropies has been discussed in the condensed matter physics; for example, see Ref. [37]. In QCD, such a relation is not clear, but it is an interesting direction to confirm the topological nature of the transition. The calculation of the entanglement entropy in QCD is possible by using the lattice QCD simulation, and pioneering works are found in Refs. [38–40] in the quenched case. The calculation with the dynamical quark will provide us information to confirm present discussions.

Using the perturbative expansion in terms of μ_R, we have investigated the behavior of T_{RW} at small μ_R and then the decreasing behavior of T_{RW} is obtained. Based on these results, we presented two scenarios of the QCD phase diagram at finite complex chemical potential. First scenario which is the correlated case has the strong correlation between the chiral and deconfinement transitions. The RW endpoint at finite μ_R finally reaches the chiral transition surface. Then, the critical point can become more complex than the usual expectation since two more first order transition lines can be connected at the critical point. The second scenario is the uncorrelated case. The RW endpoint is separated from the chiral transition surface.

Since the complex chemical potential is related with the Lee–Yang zero analysis and the analytic continuation to the finite μ_R region, understanding of the QCD phase structure at finite complex chemical potential may have impact on the beam energy scan program in heavy ion collider experiments, investigation of neutron star structures and so on. Our results are based on perturbative calculations and thus the non-perturbative checks should be done.

K.K. thanks Hiroaki Kouno, Keitaro Nagata and Masanobu Yahiro for useful discussions and comments. He is especially thankful to Yoshimasa Hidaka for his comment which motivates us to start this study. K.K. is supported by Grants-in-Aid for Japan Society for the Promotion of Science (JSPS) fellows (No. 26-1717). A.O. is supported in part by KAKENHI (Nos. 23340067, 24340054, 24540271, 15K05079, 24105001, 24105008), and by the Yukawa International Program for Quark-Hadron Sciences.

References

[1] P. de Forcrand, Simulating QCD at finite density, PoS LAT2009 (2009) 010, arXiv:1005.0539.
[2] Y. Sakai, K. Kashiwa, H. Kouno, M. Yahiro, Phase diagram in the imaginary chemical potential region and extended Z(3) symmetry, Phys. Rev. D 78 (2008) 036001, http://dx.doi.org/10.1103/PhysRevD.78.036001, arXiv:0803.1902.
[3] K. Kashiwa, M. Matsuzaki, H. Kouno, Y. Sakai, M. Yahiro, Meson mass at real and imaginary chemical potentials, Phys. Rev. D 79 (2009) 076008, http://dx.doi.org/10.1103/PhysRevD.79.076008, arXiv:0812.4747.
[4] A. Roberge, N. Weiss, Gauge theories with imaginary chemical potential and the phases of QCD, Nucl. Phys. B 275 (1986) 734, http://dx.doi.org/10.1016/0550-3213(86)90582-1.
[5] X. Wen, Topological order in rigid states, Int. J. Mod. Phys. B 4 (1990) 239, http://dx.doi.org/10.1142/S0217979290000139.
[6] M. Sato, Topological discrete algebra, ground state degeneracy, and quark confinement in QCD, Phys. Rev. D 77 (2008) 045013, http://dx.doi.org/10.1103/PhysRevD.77.045013, arXiv:0705.2476.
[7] M. D'Elia, F. Sanfilippo, The order of the Roberge–Weiss endpoint (finite size transition) in QCD, Phys. Rev. D 80 (2009) 111501, http://dx.doi.org/10.1103/PhysRevD.80.111501, arXiv:0909.0254.
[8] C. Bonati, G. Cossu, M. D'Elia, F. Sanfilippo, The Roberge–Weiss endpoint in $N_f = 2$ QCD, Phys. Rev. D 83 (2011) 054505, http://dx.doi.org/10.1103/PhysRevD.83.054505, arXiv:1011.4515.
[9] C. Bonati, P. de Forcrand, M. D'Elia, O. Philipsen, F. Sanfilippo, Chiral phase transition in two-flavor QCD from an imaginary chemical potential, Phys. Rev. D 90 (7) (2014) 074030, http://dx.doi.org/10.1103/PhysRevD.90.074030, arXiv:1408.5086.

[10] Y. Nishida, Phase structures of strong coupling lattice QCD with finite baryon and isospin density, Phys. Rev. D 69 (2004) 094501, http://dx.doi.org/10.1103/PhysRevD.69.094501, arXiv:hep-ph/0312371.
[11] N. Kawamoto, K. Miura, A. Ohnishi, T. Ohnuma, Phase diagram at finite temperature and quark density in the strong coupling limit of lattice QCD for color SU(3), Phys. Rev. D 75 (2007) 014502, http://dx.doi.org/10.1103/PhysRevD.75.014502, arXiv:hep-lat/0512023.
[12] R. Garcia Martin, J. Pelaez, Chiral condensate thermal evolution at finite baryon chemical potential within chiral perturbation theory, Phys. Rev. D 74 (2006) 096003, http://dx.doi.org/10.1103/PhysRevD.74.096003, arXiv:hep-ph/0608320.
[13] A. Ayala, A. Bashir, C. Dominguez, E. Gutierrez, M. Loewe, et al., QCD phase diagram from finite energy sum rules, Phys. Rev. D 84 (2011) 056004, http://dx.doi.org/10.1103/PhysRevD.84.056004, arXiv:1106.5155.
[14] D.J. Gross, R.D. Pisarski, L.G. Yaffe, QCD and instantons at finite temperature, Rev. Mod. Phys. 53 (1981) 43, http://dx.doi.org/10.1103/RevModPhys.53.43.
[15] N. Weiss, The effective potential for the order parameter of Gauge theories at finite temperature, Phys. Rev. D 24 (1981) 475, http://dx.doi.org/10.1103/PhysRevD.24.475.
[16] Y. Aharonov, D. Bohm, Significance of electromagnetic potentials in the quantum theory, Phys. Rev. 115 (1959) 485–491, http://dx.doi.org/10.1103/PhysRev.115.485.
[17] H. Kouno, Y. Sakai, K. Kashiwa, M. Yahiro, Roberge–Weiss phase transition and its endpoint, J. Phys. G 36 (2009) 115010, http://dx.doi.org/10.1088/0954-3899/36/11/115010, arXiv:0904.0925.
[18] P. de Forcrand, O. Philipsen, The QCD phase diagram for small densities from imaginary chemical potential, Nucl. Phys. B 642 (2002) 290–306, http://dx.doi.org/10.1016/S0550-3213(02)00626-0, arXiv:hep-lat/0205016.
[19] K. Fukushima, Chiral effective model with the Polyakov loop, Phys. Lett. B 591 (2004) 277–284, http://dx.doi.org/10.1016/j.physletb.2004.04.027, arXiv:hep-ph/0310121.
[20] K. Fukushima, Y. Hidaka, A model study of the sign problem in the mean-field approximation, Phys. Rev. D 75 (2007) 036002, http://dx.doi.org/10.1103/PhysRevD.75.036002, arXiv:hep-ph/0610323.
[21] H. Nishimura, M.C. Ogilvie, K. Pangeni, Complex saddle points in QCD at finite temperature and density, arXiv:1401.7982.
[22] H. Nishimura, M.C. Ogilvie, K. Pangeni, Complex saddle points and disorder lines in QCD at finite temperature and density, arXiv:1411.4959.
[23] Y. Tanizaki, H. Nishimura, K. Kashiwa, Evading the sign problem in the mean-field approximation through Lefschetz-thimble path integral, arXiv:1504.02979.
[24] E. Witten, Analytic continuation of Chern–Simons theory, arXiv:1001.2933, 2010, pp. 347–446.
[25] M. Cristoforetti, F. Di Renzo, L. Scorzato, New approach to the sign problem in quantum field theories: high density QCD on a Lefschetz thimble, Phys. Rev. D 86 (2012) 074506, http://dx.doi.org/10.1103/PhysRevD.86.074506, arXiv:1205.3996.
[26] H. Fujii, D. Honda, M. Kato, Y. Kikukawa, S. Komatsu, et al., Hybrid Monte Carlo on Lefschetz thimbles – a study of the residual sign problem, J. High Energy Phys. 1310 (2013) 147, http://dx.doi.org/10.1007/JHEP10(2013)147, arXiv:1309.4371.
[27] G. Parisi, Y.-s. Wu, Perturbation theory without Gauge fixing, Sci. Sinter. 24 (1981) 483.
[28] G. Parisi, On complex probabilities, Phys. Lett. B 131 (1983) 393–395, http://dx.doi.org/10.1016/0370-2693(83)90525-7.
[29] M. D'Elia, M.-P. Lombardo, Finite density QCD via imaginary chemical potential, Phys. Rev. D 67 (2003) 014505, http://dx.doi.org/10.1103/PhysRevD.67.014505, arXiv:hep-lat/0209146.
[30] C. Sasaki, B. Friman, K. Redlich, Susceptibilities and the phase structure of a chiral model with Polyakov loops, Phys. Rev. D 75 (2007) 074013, http://dx.doi.org/10.1103/PhysRevD.75.074013, arXiv:hep-ph/0611147.
[31] K. Kashiwa, H. Kouno, M. Matsuzaki, M. Yahiro, Critical endpoint in the Polyakov-loop extended NJL model, Phys. Lett. B 662 (2008) 26–32, http://dx.doi.org/10.1016/j.physletb.2008.01.075, arXiv:0710.2180.
[32] A. Nakamura, K. Nagata, Probing QCD phase structure by Baryon multiplicity distribution, arXiv:1305.0760.
[33] K. Nagata, K. Kashiwa, A. Nakamura, S.M. Nishigaki, Lee–Yang zero distribution of high temperature QCD and Roberge–Weiss phase transition, arXiv:1410.0783.
[34] C.-N. Yang, T. Lee, Statistical theory of equations of state and phase transitions. 1. Theory of condensation, Phys. Rev. 87 (1952) 404–409, http://dx.doi.org/10.1103/PhysRev.87.404.
[35] T. Lee, C.-N. Yang, Statistical theory of equations of state and phase transitions. 2. Lattice gas and Ising model, Phys. Rev. 87 (1952) 410–419, http://dx.doi.org/10.1103/PhysRev.87.410.
[36] K. Kashiwa, T.-G. Lee, K. Nishiyama, R. Yoshiike, Inhomogeneous chiral condensates and non-analyticity under an external magnetic field, arXiv:1507.08382.
[37] M. Levin, X.-G. Wen, Detecting topological order in a ground state wave function, Phys. Rev. Lett. 96 (2006) 110405, http://dx.doi.org/10.1103/PhysRevLett.96.110405.
[38] P.V. Buividovich, M.I. Polikarpov, Numerical study of entanglement entropy in SU(2) lattice gauge theory, Nucl. Phys. B 802 (2008) 458–474, http://dx.doi.org/10.1016/j.nuclphysb.2008.04.024, arXiv:0802.4247.
[39] Y. Nakagawa, A. Nakamura, S. Motoki, V.I. Zakharov, Entanglement entropy of SU(3) Yang–Mills theory, PoS LAT2009 (2009) 188, arXiv:0911.2596.
[40] Y. Nakagawa, A. Nakamura, S. Motoki, V.I. Zakharov, Quantum entanglement in SU(3) lattice Yang–Mills theory at zero and finite temperatures, PoS LATTICE2010 (2010) 281, arXiv:1104.1011.